

LIST OF PUBLICATIONS

- 1) "Synthesis and Characterization Studies of Homopolymers of N-Vinyl Pyrrolidone, Vinyl Acetate and Their Copolymers", **Ismail Mathakiya**, and A.K.Rakshit, *J. Appl. Polym. Sci.*, **68**, 91 (1998).
- 2) "Terpolymerization of Acrylamide, Acrylic Acid and Acrylonitrile : Synthesis and Properties", **Ismail Mathakiya**, Veena Vangani and A.K.Rakshit, *J. Appl. Polym. Sci.*, **69**, 217 (1998).
- 3) "Synthesis of N-Vinyl Pyrrolidone - Vinyl Acetate Copolymers in Microemulsion Medium : Spectroscopic Characterization of the Polymers", **Ismail Mathakiya**, P.V.C.Rao and A.K.Rakshit, *IUPAC Int. Symp. Adv. Polym. Sci. Techno.*, **2**, 929 (1998).
- 4) "Studies of Thermal Analysis of Homopolymers of Acrylamide, Acrylic Acid Acrylonitrile and Their Terpolymers", **Ismail Mathakiya** and A.K.Rakshit, *Proceedings of the 11th National Symposium on Thermal Analysis*, (1998) p.212.
- 5) "Studies of Properties of N-Vinyl Pyrrolidone - Vinyl Acetate Copolymers and Their Hydrolysed Products", **Ismail Mathakiya**, C.F.Desai and A.K.Rakshit, *Int. Symp. on Polymers Beyond AD 2000* (1999) p.322.
- 6) "Tercopolymers of Acrylamide, Acrylic Acid, Acrylonitrile : Further Characterization and Biodegradation Studies", Bragadish Iyer, **Ismail Mathakiya**, Avinash K. Shah and A.K.Rakshit - *Polym. International* (accepted for publication).
- 7) "Synthesis and Characterization of Styrene-Acrylic Esters Copolymers", **Ismail Mathakiya**, P.V.C.Rao and A.K.Rakshit - submitted to *J. Appl. Polym. Sci.*
- 8) "Preparation, Characterization of Properties of Vinyl Acetate and Acrylic Esters Polymers", **Ismail Mathakiya**, P.V.C.Rao and A.K.Rakshit - submitted to *Macromolecular Chemistry & Physics*.

Terpolymerization of Acrylamide, Acrylic Acid, and Acrylonitrile: Synthesis and Properties

ISMAIL MATHAKIYA, VEENA VANGANI, ANIMESH KUMAR RAKSHIT

Chemistry Department, Faculty of Science, M S University, Baroda 390002, India

Received 27 May 1997, accepted 3 September 1997

ABSTRACT: Free-radical solution terpolymerization of acrylamide, acrylic acid, and acrylonitrile was carried out in a mixture of dimethylformamide and water (60/40, v/v) at 85°C using benzoyl peroxide as the initiator. The polymers were characterized by elemental analysis, IR, ¹H-NMR, TGA, and viscosity measurements. Elemental analysis data were used to evaluate the terpolymer composition. The reactivity ratios were determined by Fineman–Ross and Kelen–Tudos methods. The reactivity ratios (r) for the copolymerization of (1) acrylic acid + acrylonitrile with (2) acrylamide was found to be $r_1 = 0.86 \pm 0.09$ and $r_2 = 1.93 \pm 0.03$, respectively, by the Kelen–Tudos method. The Fineman–Ross method yielded a value of $r_1 = 0.86 \pm 0.05$ and $r_2 = 1.94 \pm 0.09$, respectively. The activation energy values for various stages of decomposition were calculated from TGA analysis. Voluminosity (V_E) and the shape factor (ν) were also computed from the viscosity measurements in different ratios of the solvent mixture. © 1998 John Wiley & Sons, Inc. *J Appl Polym Sci* 69: 217–228, 1998

Key words: terpolymers, synthesis, properties; reactivity ratio

INTRODUCTION

Research on polymers has been mainly addressed to the synthesis of new materials with specific performance for last 30 years. A wide variety of chemical or physical strategies including copolymerization, polymer blends and composites, or crosslinking networks have been explored to match the individual requirements.¹ Terpolymerizations have continued to evoke interest by both academics and industrialists. One of the main advantages of this technique is that it provides a convenient method of synthesizing new polymeric structures with wide ranges of properties.² Although extensive literature is available for homo- and copolymerization, very little kinetic or synthetic information is available for terpolymerization.³ As it becomes more and more possible to

“tailor-make” polymers with specific physical and chemical properties, it will undoubtedly become necessary to resort to such multiple combinations wherein each monomer contributes some particular property or properties.

Interest in multifunctional synthetic polymers or copolymers is steadily increasing, as macromolecular catalysts, macromolecular drugs, or antimetastatic agents.⁴ Such activated drug-binding matrices are usually based on *N*-acryloyloxyphthalimide and *N*-methacryloyloxyphthalimide with methyl acrylate and acrylonitrile as comonomers. The terpolymerization of maleic anhydride–methyl methacrylate–styrene has been studied extensively and modified by tributyltin oxide to yield terpolymers of biological interest.⁵ The growth in the production of plastic materials during the past few years has been accompanied by an increased demand for materials with improved physical and mechanical properties, greater heat and radiation stability, etc. Only a few homopolymers answer such demands. In this respect, the terpolymerization of acrylonitrile, styrene, and esters of α -cyanocinnamic acid has been

Correspondence to: A. K. Rakshit

Contract grant sponsor: Department of Biotechnology, Government of India

Journal of Applied Polymer Science, Vol. 69, 217–228 (1998)

© 1998 John Wiley & Sons, Inc.

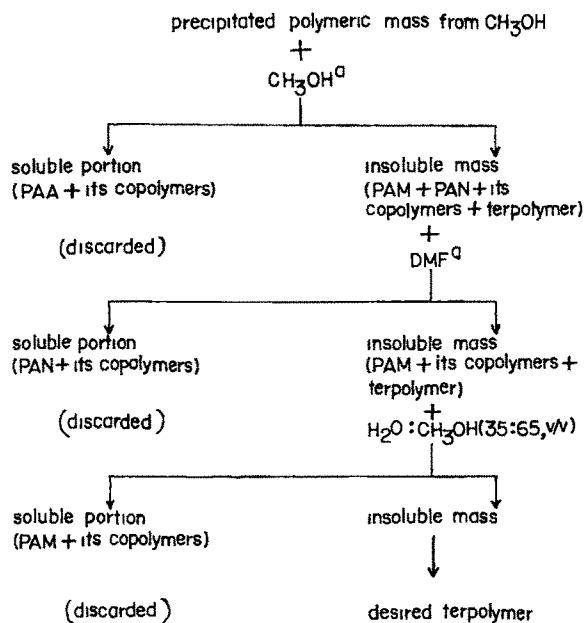
CCC 0021-8995/98/020217-12

reported.⁶ Recently, the water uptake and swelling behavior of physically crosslinked, inhomogeneous poly(acrylonitrile–acrylamide–acrylic acid) hydrogels have been reported.⁷ In this article, we report on the synthesis and properties of terpolymers of acrylamide, acrylonitrile, and acrylic acid from various feed ratios. The changes in the physical and chemical properties as a function of the chemical composition are studied and presented in detail.

EXPERIMENTAL

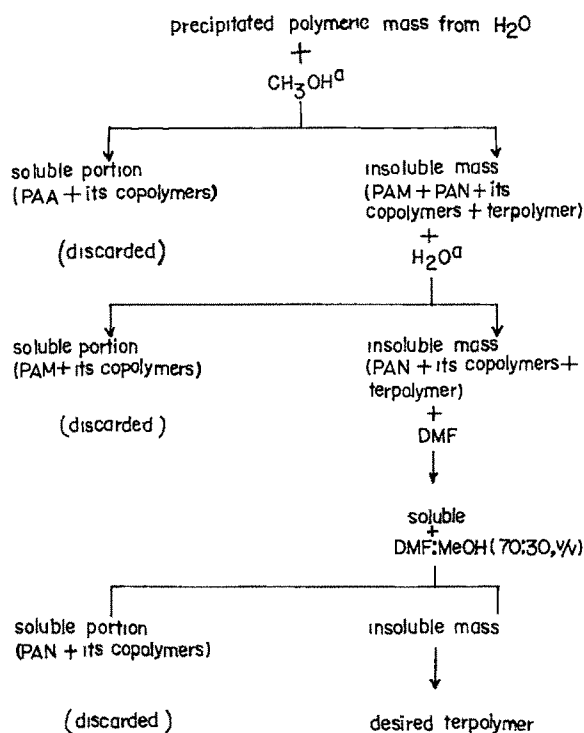
Acrylamide (Mitsubishi Chemicals Ltd), acrylic acid (National Chemicals, Baroda, India), and acrylonitrile (BDH, Poole, England) were used for the polymerization without any prior purification. Benzoyl peroxide (National Chemicals, Baroda, India) was purified by dissolving it in chloroform at room temperature and reprecipitating it by adding methanol, before it used for the polymerization. Hydrogen peroxide (Glaxo, Mumbai, India, 100 vol, i.e., 30% w/v) was used as received. The solvents were freshly distilled prior to use.

IR spectra of the films of the homopolymers and terpolymers were recorded on a Perkin–Elmer 16PC spectrophotometer. The films were prepared by dissolving the polymer in a mixture of DMF : H₂O (60 : 40, v/v) and pouring the solution



^a soxhlet extraction

Figure 1 Schematic representation of purification of terpolymers I and II



^a soxhlet extraction

Figure 2 Schematic representation of purification of terpolymers III and IV.

over a pool of mercury. The films were obtained by vacuum evaporation of the solvent.

The NMR of the polymer solutions were recorded on a JEOL GSX, 400 MHz for PMR at the RSIC, IIT, Madras, India. Elemental analysis was done on a Haraeus, RAPID (made in Germany) C, H, N, O, analyzer at S.P. University, Vallabh Vidyanagar, India.

TGA was recorded with a Shimadzu thermal analyzer DT-30B. The TGA analysis was done under a nitrogen atmosphere. Viscosity studies of different solutions were carried out with the help of an Ubbelohde viscometer, placed vertically in a thermostat, at all required temperatures ($\pm 0.05^\circ\text{C}$).

The synthesis of terpolymers was carried out in various monomer feed ratios of (I) 80 : 10 : 10, (II) 60 : 20 : 20, (III) 40 : 30 : 30, and (IV) 20 : 40 : 40 (w/w/w) of acrylamide (AM), acrylic acid (AA), and acrylonitrile (AN), respectively. The solution polymerization was carried out in a mixture of DMF and water (60 : 40, v/v) under a nitrogen atmosphere. The monomer-to-solvent ratio was 1 : 4 (w/v). The initiator benzoyl peroxide concentration was 1.0% (w/w) to total monomer weight. The reactor setup consisted of a three-

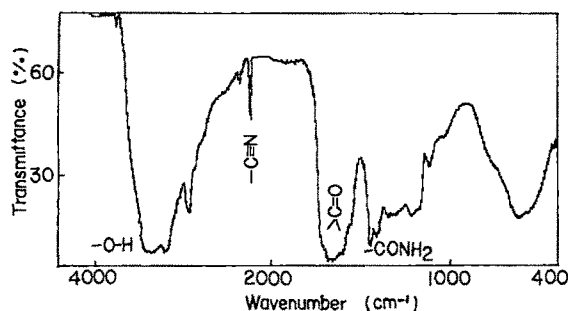


Figure 3 Representative IR spectrum of terpolymer II

necked round-bottom flask equipped with a water condenser at one side neck and the N_2 inlet at the other. The reaction mixture was mechanically stirred through the center neck. The whole assembly was placed in a thermostated water bath at 85°C . The reaction time was 8 h. After polymerization, the reaction mass, for samples I and II, was poured into an excess of methanol, and for samples III and IV, it was poured into an excess of distilled water. The reprecipitated products were Soxhlet-extracted with various solvents to remove the respective homo- and copolymers. The purification procedure of samples I and II is schematically shown in Figure 1, and that of samples III & IV is shown in Figure 2.

The synthesis of the homopolymers polyacrylic acid (PAA)⁸ and polyacrylamide (PAM)^{9,10} was done as reported in the literature. The synthesis of polyacrylonitrile (PAN) was carried out as reported earlier.^{11,12} All the homo- and terpolymers were dried *in vacuo* and then characterized.

RESULTS AND DISCUSSION

The homopolymers PAM, PAN, and PAA showed characteristic IR absorptions which agreed very well with those reported in the literature. PAN

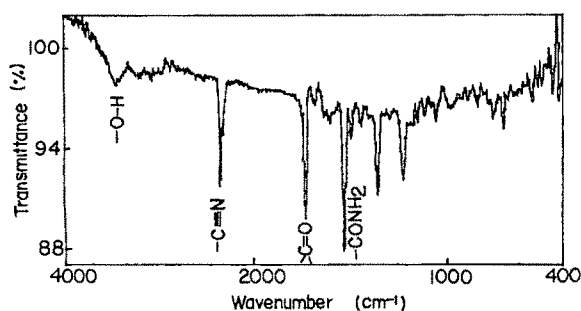


Figure 4 Representative IR spectrum of terpolymer III

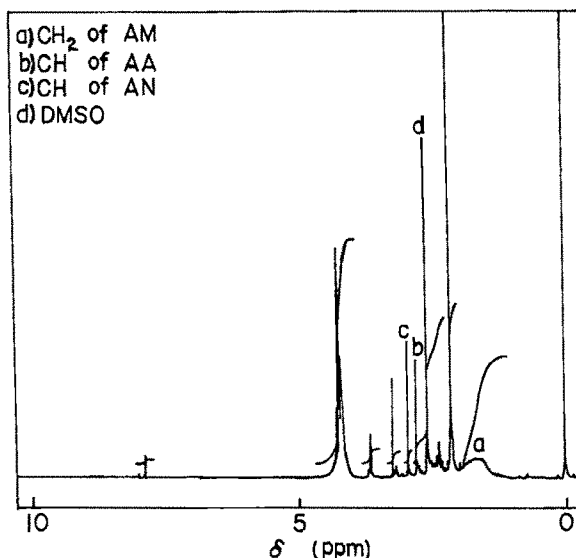


Figure 5 ^1H -NMR spectrum of terpolymer II

showed strong absorptions at 2246 and 1452 cm^{-1} due to the nitrile group. The $\text{C}=\text{O}$ band of PAA was observed at 1738 cm^{-1} . Besides this, the broad absorption band due to the $\text{O}-\text{H}$ of the $-\text{COOH}$ group was observed around 3300 cm^{-1} . The IR spectrum of PAM showed strong absorption at 1650 cm^{-1} due to the $\text{C}=\text{O}$ bond of the carbonamide group. The medium absorption at 1400 cm^{-1} was due to the $\text{C}-\text{N}$ stretch. Representative IR spectra of terpolymers II (AM-AA-AN = $60:20:20$) and III (AM-AA-AN = $40:30:30$) are given in Figures 3 and 4. The characteristic absorption peaks due to the three functional groups were present in all the terpolymers studied.

Further evidence for the three monomers incor-

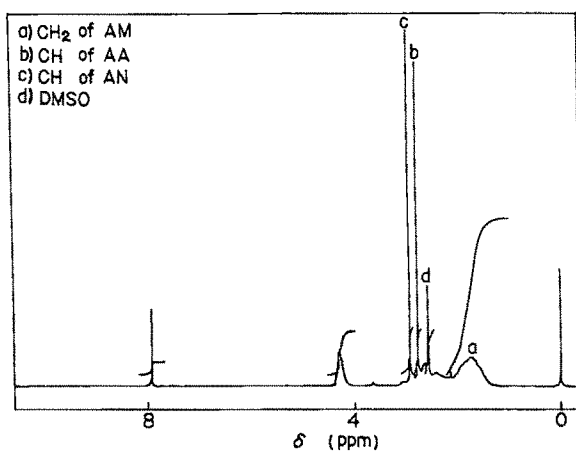


Figure 6 ^1H -NMR spectrum of terpolymer III

Table I Composition of AM, AA, and AN in Feed and in Terpolymers

Samples	Mol Fraction (<i>M</i>) of AM, AA, and AN in Feed			Elemental Analysis		Mol Fraction (\emptyset) of AM, AA, and AN in Terpolymer (Experimental)		
	(<i>M</i> _{AM})	(<i>M</i> _{AA})	(<i>M</i> _{AN})	N (%)	O (%)	(\emptyset _{AM})	(\emptyset _{AA})	(\emptyset _{AN})
I AM-AA-AN (80 10 10)	0.775	0.096	0.130	17.14	25.31	0.861	0.130	0.009
II AM-AA-AN (60 20 20)	0.563	0.185	0.251	17.27	22.18	0.568	0.179	0.254
III AM-AA-AN (40 30 30)	0.364	0.270	0.366	14.91	24.76	0.446	0.291	0.262
IV AM-AA-AN (20 40 40)	0.177	0.349	0.474	14.08	23.61	0.224	0.358	0.417
PAM	—	—	—	18.12	25.61	—	—	—
PAN	—	—	—	25.39	—	—	—	—

porated was given by the ¹H-NMR spectra of the terpolymers. In the ¹H-NMR spectra of PAM, the methylene protons appeared as a broad peak at $\delta = 1.6\text{--}1.8$ ppm.¹³ The methine protons resonate at $\delta = 2.28$ ppm. The ¹H-NMR spectrum of PAN shows peaks at $\delta = 2.071$ ppm due to methylene protons and due to methine protons at $\delta = 3.122$ ppm. In the presence of monomer AA, the methylene signal shifted downfield to $\delta = 2.056$; the methine proton also showed a shift to $\delta = 3.120$ ppm.¹⁴ In the case of terpolymers (Figs. 5 and 6), a broad peak appeared in the range of $\delta = 1.4\text{--}2.0$ due to methylene groups of AM. A sharp peak was observed due to the methine of the AA comonomer at $\delta = 2.75$ ppm and at $\delta = 2.93$ due to the AN comonomer. As the ratio of AA and AN increases, the intensity of the peak height increases in the expected direction.

The experimental feed ratios of various monomers as well as the composition of the resulting terpolymers, obtained by elemental analysis, are summarized in Table I. The reactivity ratios (*r*)

of (AA + AN) and AM in the terpolymer were estimated by the graphical method of Kelen-Tudos¹⁵:

$$\theta = r_1\epsilon - \frac{r_2(1 - \epsilon)}{\gamma} \quad (1)$$

where 1 stands for (AA + AN) and 2 for AM. θ , ϵ , and γ are mathematical functions of *G* and *F* as defined in Table II. On plotting θ versus ϵ , a linear plot was obtained. The intercepts at $\epsilon = 0$ and $\epsilon = 1$ gave $-r_2/\gamma$ and r_1 , respectively. The values obtained for r_1 and r_2 were $r_1 = 0.86 \pm 0.09$ and $r_2 = 1.93 \pm 0.03$.

The reactivity ratios r_1 and r_2 were also determined by the Fineman-Ross^{16,17} method. The following equation was used:

$$X(Y - 1)/Y = r_1X^2/Y - r_2 \quad (2)$$

where $X = M_1/M_2$ and $Y = \frac{\emptyset_1}{\emptyset_2}$ (as defined in Table II)

Table II Kelen-Tudos Parameters for AM and for AA + AN

Samples	$X = \frac{M_1}{M_2}$	$Y = \frac{\emptyset_1}{\emptyset_2}$	$G = \frac{X(Y - 1)}{Y}$	$F = \frac{X^2}{Y}$	$\epsilon = \frac{F}{\gamma + F}$	$\theta = \frac{G}{\gamma + F}$
I	0.29	0.16	-1.51	0.53	0.23	-0.65
II	0.77	0.76	—	—	—	—
III	1.75	1.24	0.34	2.46	0.58	0.08
IV	4.65	3.46	3.31	6.25	0.77	0.41

$\gamma = \sqrt{F_{\max}F_{\min}} = 1.81$, M_1 is the mol fraction of AA + AN and M_2 is the mol fraction of AM in feed, \emptyset_1 and \emptyset_2 are their respective experimental mol fractions in the terpolymer

Table III Structural Data for the Terpolymers of AM and of AA + AN

Samples	Composition ^a (Mol Fraction)		Blockiness ^b (Mol Fraction)		Alternation ^b (Mol Fraction)	Mean Sequence Length		$\frac{\mu_1}{\mu_2}$
	ϕ_1	ϕ_2	1-1 (X')	2-2 (Y')	1-2 (Z')	μ_1	μ_2	
I	0.14	0.86	0.028	0.748	0.224	1.1	12.9	0.1
II	0.43	0.57	0.215	0.355	0.429	1.6	3.6	0.5
III	0.55	0.45	0.333	0.233	0.433	2.1	2.6	0.8
IV	0.78	0.22	0.624	0.064	0.311	4.1	1.5	2.6

^a From elemental analysis^b Statistically calculated using reactivity ratios

On plotting $X(Y - 1)/Y$ against X^2/Y , a straight line was obtained, whose slope was r_1 and the intercept yielded r_2 . The values obtained for r_1 and r_2 are 0.86 ± 0.05 and 1.94 ± 0.09 , respectively. The $r_1 r_2$ value indicates that the terpolymers are block copolymers of AM and (AA + AN) which are rich in AM.¹⁷

The statistical distributions of the monomer sequences 1-1, 2-2, and 1-2 were calculated using the following relations¹⁸⁻²⁰.

$$X' = \theta_1 - 2\phi_1\phi_2 / \{1 + [(2\phi_1 - 1)^2 + 4r_1r_2\phi_1\phi_2]^{1/2}\} \quad (3)$$

$$Y' = \theta_2 - 2\phi_1\phi_2 / \{1 + [(2\phi_1 - 1)^2 + 4r_1r_2\phi_1\phi_2]^{1/2}\} \quad (4)$$

$$Z' = 4\phi_1\phi_2 / \{1 + [(2\phi_1 - 1)^2 + 4r_1r_2\phi_1\phi_2]^{1/2}\} \quad (5)$$

where ϕ_1 is the mol fraction of AA and AN together and ϕ_2 is the mol fraction of AM when the blockiness between these are considered in the terpolymers. The mol fractions of 1-1, 2-2, and 1-2 are designated by X' , Y' , and Z' , as listed in Table III. The mean sequence lengths μ_1 and μ_2 were calculated utilizing the relations

$$\mu_1 = 1 + r_1(\phi_1)/(\phi_2) \quad (6)$$

$$\mu_2 = 1 + r_2(\phi_2)/(\phi_1) \quad (7)$$

The calculated values are listed in Table III

The TGA of PAM, PAA, PAN, and terpolymer

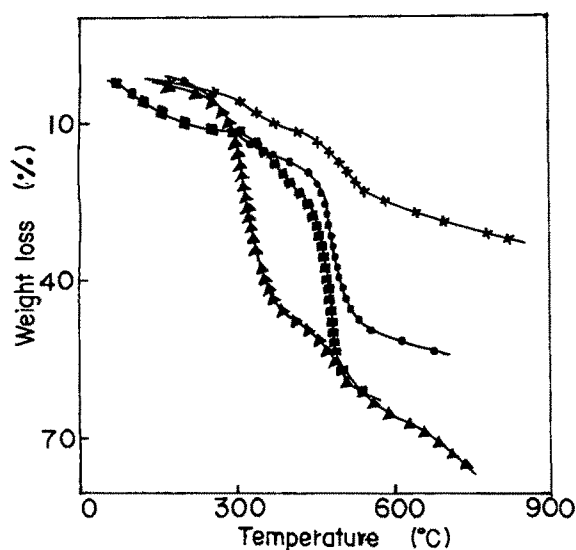


Figure 7 Representative TGA plots of (■) PAM, (▲) PAA, (X) PAN, and (●) terpolymer IV at heating rate of 10 K min^{-1} in N_2 atmosphere

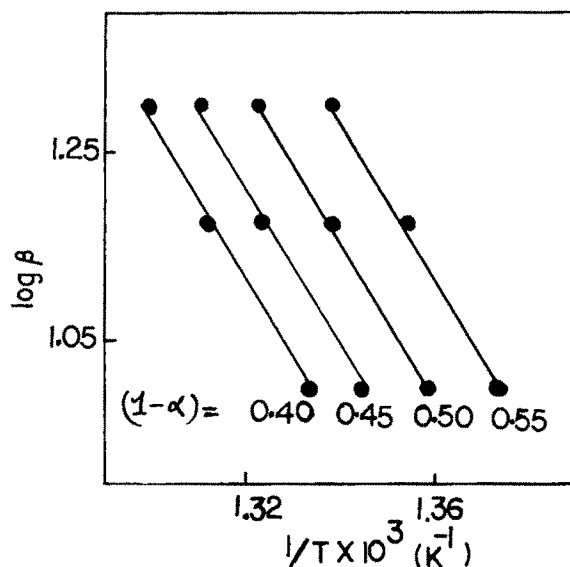


Figure 8 Representative Ozawa plot of $\log \beta$ against $1/T$ for terpolymer IV at different $(1 - \alpha)$ values (see text)

Table IV Activation Energies of Decomposition of Various Homopolymers and Terpolymers (Ozawa Method, See Text)

Polymer Samples		Activation Energy, (E) (kJ mol ⁻¹) (1 - α) ^a			
I	AM-AA-AN	61.4	63.6	63.1	60.8
	(80 : 10 : 10)	(0.20)	(0.30)	(0.35)	(0.40)
II	AM-AA-AN	66.1	62.4	59.7	55.5
	(60 : 20 : 20)	(0.20)	(0.25)	(0.30)	(0.35)
III	AM-AA-AN	60.3	57.9	55.3	55.3
	(40 : 30 : 30)	(0.30)	(0.35)	(0.40)	(0.45)
IV	AM-AA-AN	168.8	160.4	152.5	156.9
	(20 : 40 : 40)	(0.40)	(0.45)	(0.50)	(0.55)
	PAM	70.4	70.4	71.3	68.6
		(0.25)	(0.30)	(0.35)	(0.40)
	PAA	69.9	67.5	70.2	67.7
		(0.55)	(0.60)	(0.65)	(0.70)
	PAN	112.1	119.4	112.0	112.0
		(0.20)	(0.30)	(0.35)	(0.40)

^a Values of (1 - α) are given in parentheses

IV are given in Figure 7. The thermogram of terpolymer IV falls in between those of its homopolymers, indicating a somewhat intermediate thermal stability. Other terpolymers also show in-

termediate thermal stability. Two-stage decomposition was observed in all cases, except PAM. The first-stage decomposition of PAA started around 260°C. This is due to the formation of anhydride linkages. Similar values were reported earlier for PAA.²¹ Heating above 350°C results in rapid decomposition to monomer, carbon dioxide, and volatile hydrocarbons. The TGA of PAM was three-staged, as observed before.²² First, the loss of water which is nonstoichiometric occurred. This is followed by the subsequent loss of ammonia and other gaseous products from the PAN structure formed during the decomposition of PAM and partly from the remaining PAM in the course of heating to 600°C.²³

The Ozawa²⁴⁻²⁶ method, a dynamic analysis technique, was used for the determination of the activation energy. Thermograms were recorded at various heating rates of 10, 15, and 20 K min⁻¹ in N₂. The fraction of decomposition, α , was obtained by the following equation.

$$\alpha = (W_0 - W_t)/(W_0 - W_f) \quad (8)$$

where W_0 is the initial weight of the polymer, W_t , the weight of the polymer at temperature t ; and W_f , the final weight. The (1 - α) values were found for each heating rate from the TG curves, the (1 - α) values, hence, obtained were plotted against $1/T$. According to the Ozawa method,²⁴⁻²⁶

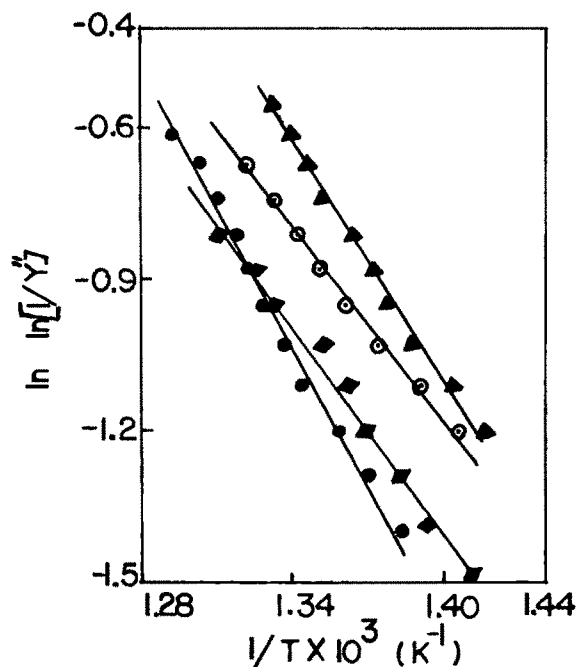
**Figure 9** Brodie plot for terpolymers (▲) I, (○) II, (■) III, (●) IV (see text)

Table V Activation Energy of Decomposition for Various Homopolymers and Terpolymers in Different Ratios by Thermogravimetric Analysis

Polymer Samples	Decomposition Temperature Range (°C)	Weight Loss (%)	Activation Energy ^a (kJ mol ⁻¹)
AM AA AN (80 10 · 10) I	190–425	24	18 0
	433–478	44	65 1
AM AA AN (60 20 20) II	214–399	20	19 9
	439–489	40	48 9
AM AA AN (40 30 30) III	205–410	16	20 3
	436–490	36	58.8
AM AA AN (20 40 40) IV	198–326	14	32 7
	450–501	42	75 0
PAM	70–204	10	20 3
	305–420	24	23.5
	435–495	58	89 2
PAA	260–359	42	66 0
	435–660	70	13 0
PAN	305–473	16	20 3
	520–844	36	11.8

^a Calculated using Broido's method at a heating rate of 10°C/min in N₂ atmosphere

the plot of $\log \beta$ (where β is the heating rate) against the reciprocal of absolute temperature, for different values of $(1 - \alpha)$, is linear. The activation energy (E) of the decomposition was obtained from the slope of above linear plot,^{24–26} using the equation

$$\text{Slope} = -0.4567 (E/R) \quad (9)$$

The plot of $\log \beta$ versus $1/T$, for terpolymer IV at different values of $(1 - \alpha)$, each differing by 0.05, is shown in Figure 8. The activation energy at different $(1 - \alpha)$ are given in Table IV. For terpolymers, the activation energy of decomposition varied with $(1 - \alpha)$. For homopolymers, the activation energy was independent of the fraction of decomposition. In terpolymer IV, where the AA and AN feed ratios are higher, the E values are much higher than the rest, indicating a synergistic effect on its stability. A high stability of PAN in a nitrogen atmosphere was observed. The PAA and PAM have almost the same stability though lower than PAN in the presence of nitrogen.

The activation energy associated with each stage of decomposition was also evaluated by the well-known Broido method.¹² The equation used for the calculation of activation energy (E) was

$$\ln \ln (1/Y'') = (-E/R)(1/T) + \text{constant} \quad (10)$$

where

$$Y'' = (W_t - W_\infty)/(W_0 - W_\infty) \quad (11)$$

that is, Y'' is the fraction of the number of initial molecules not yet decomposed; W_t , the weight at any time t ; W_∞ , the weight at infinite time (= zero); and W_0 , the initial weight. A plot of $\ln \ln (1/Y'')$ versus $1/T$ [eq. (10)] gives an excellent approximation to a straight line over a range of $0.999 > Y'' > 0.001$. The slope is related to the activation energy. Representative plots are shown in Figure 9. The calculated values for the activation energy of decomposition are listed in Table V. The terpolymers show two-stage decomposition even where AM is 80% in the feed ratio, although the homopolymer PAM shows three-stage decomposition. The first stage of PAM decomposition is not seen in terpolymer decompositions. In general, terpolymers require more activation energy than do the homopolymers.

The viscosity behavior of PAM, PAN, and terpolymers I, II, III, and IV was studied at different temperatures of 30, 35, and 40°C. The viscosity studies of PAM and sets I and II were done in aqueous medium, whereas PAN and sets III and

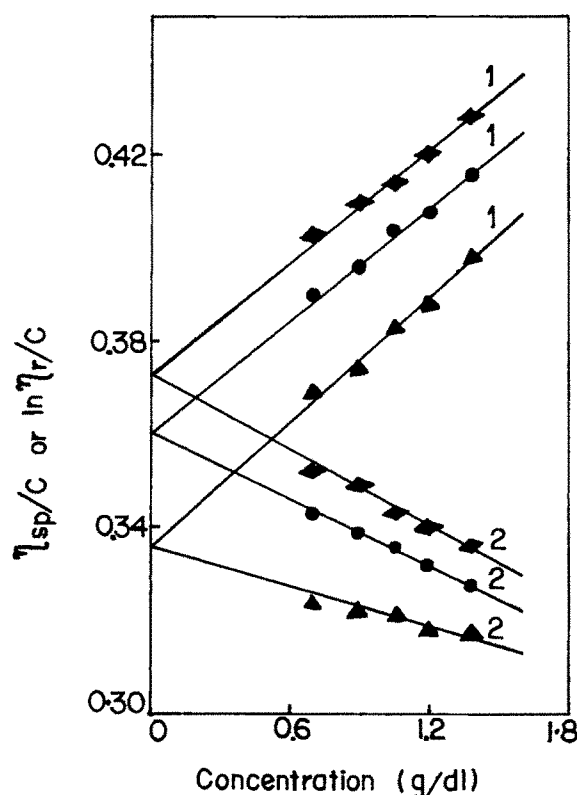


Figure 10 Typical plot of (1) η_{sp}/C and (2) $\ln \eta_r/C$ against concentration (C) for terpolymer IV (■) 30°C, (●) 35°C; (▲) 40°C

IV were done in DMF. The viscosity of all the terpolymers was also measured in mixtures of the solvents, that is, various ratios of DMF : H₂O (v/v). The intrinsic viscosity was calculated using the following equations (Huggins and Kraemer):

$$\eta_{sp}/C = [\eta] + K'[\eta]^2C \quad (12)$$

$$\ln \eta_r/C = [\eta] - K''[\eta]^2C \quad (13)$$

where K' and K'' are constants for a given polymer/solvent/temperature system. For many linear flexible polymer systems, K' often indicates the measures of the solvent power; the poorer the solvent, the higher the value of K' . The $K' - K''$ values were found to be around 0.5, as expected.^{27,28}

The η_{sp}/C values of PAM in H₂O, PAN, and set IV in DMF showed a decrease with dilution. When plotted against concentration, straight lines were obtained and intrinsic viscosity values were, hence, computed (Fig. 10). For other systems, η_{sp}/C values showed an increase with dilution, and intrinsic viscosity as well as $K' - K''$ values could not be

calculated. Intrinsic viscosities of various systems at different temperatures and some representative values of $K' - K''$ are given in Table VI.

The viscosities of various terpolymers in water, DMF, and a mixture of water · DMF, like other polyelectrolytes, showed a unique dependence on concentration.²⁹ η_{sp}/C values for the above-mentioned terpolymers increased with dilution, contrary to the behavior of nonionic polymers. Representative plots are shown in Figure 11(a). As the solution is diluted, the polymer molecules no longer fill all the space and the intervening regions extract some of the mobile ions. Net charges develop in the domains of the polymer molecule, causing them to expand. As this process continues with further dilution, the expansive forces increase. At high dilutions, polymer molecules lose most of their mobile ions and are extended virtually to their maximum length.³⁰ This leads to high values of η_{sp}/C . Such data can be satisfactorily handled through the use of the empirical relation

$$\eta_{sp}/C = A/(1 + BC^{1/2}) \quad (14)$$

where A and B are constants. A straight line was obtained on plotting $(\eta_{sp}/C)^{-1}$ against $C^{1/2}$ [Fig. 11(b)], where A represents the intrinsic viscosity $(\eta_{sp}/C)_{C \rightarrow 0}$.³⁰ The plot of $[\eta]$ against the H₂O · DMF ratio (Fig. 12) shows a maximum for all the sets of terpolymers. This indicates that at that maximum of $[\eta]$ the corresponding H₂O : DMF ratio behaves as a good solvent for the terpolymers. Relative viscosity data at different concentrations were used for calculations of the voluminosity (V_E) of the polymer solutions, at a given temperature and in different solvent systems.^{27,28,31} V_E was obtained by plotting Y against concentration C (g dL⁻¹), where (Fig. 13)

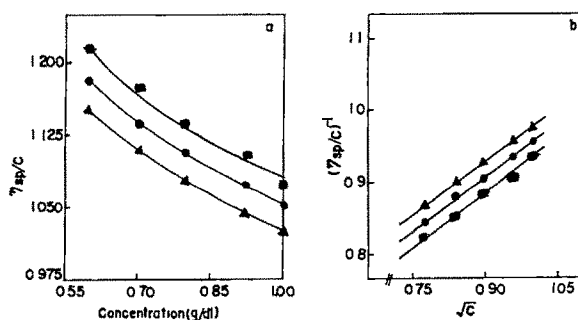


Figure 11 Plot of (a) η_{sp}/C against concentration (C) and (b) $(\eta_{sp}/C)^{-1}$ versus \sqrt{C} for terpolymer I in water (■) 30°C, (●) 35°C, (▲) 40°C

Table VI Intrinsic Viscosities of Various Polymer Systems at Different Temperatures in Various Solvents

Polymer Systems/Solvent	A or Intrinsic Viscosity $[\eta]$ (dL/g)			B			$K' - K''$ (40°C)
	30°C	35°C	40°C	30°C	35°C	40°C	
PAM/H ₂ O	—	2.98	2.91	—	—	—	0.51
Set I/H ₂ O	2.19	2.06	1.96	1.02	0.96	0.91	—
/85 : 15 H ₂ O DMF	2.17	2.11	2.09	0.88	0.87	0.88	—
/75 : 25 "	2.21	2.14	2.08	0.99	0.96	0.92	—
/40 : 60 "	2.05	2.03	1.97	1.10	1.08	1.05	—
Set II/H ₂ O	1.33	1.52	1.58	1.04	1.51	1.56	—
/85 : 15 H ₂ O DMF	1.61	1.59	1.57	1.31	1.31	1.28	—
/75 : 25 "	1.72	1.64	1.57	1.42	1.31	1.21	—
/40 : 60 "	1.70	1.59	1.54	1.23	1.33	1.11	—
Set III/DMF	1.11	0.99	0.85	1.32	1.24	0.97	—
/50 : 50 · H ₂ O DMF	1.37	1.45	1.48	0.97	1.05	1.13	—
/40 : 60 "	1.58	1.53	1.51	1.11	1.09	1.07	—
/33 : 67 "	1.57	1.53	1.41	1.07	1.09	0.90	—
/25 : 75 "	1.67	1.55	1.45	1.23	1.06	0.97	—
Set IV/DMF	0.37	0.36	0.34	—	—	—	0.48
/33 : 67 H ₂ O DMF	0.33	0.36	0.42	0.22	0.23	0.25	—
/25 : 75 "	0.41	0.35	0.34	0.30	0.09	0.09	—
/15 : 85 "	0.45	0.42	0.40	0.17	0.12	0.07	—
PAN/DMF	0.73	0.72	0.71	—	—	—	0.50

$$Y = (\eta_r^{0.5} - 1)/[C(\eta_r^{0.5} \times 1.35 - 0.1)] \quad (15)$$

$$[\eta] = \nu V_E \quad (16)$$

The straight line then obtained was extrapolated to $C = 0$ and the intercept yielded V_E . The values are listed in Table VII. The shape factor ν was calculated from the equation

The shape factor gives an idea of the shape of the macromolecules in the solution.³² The values of the shape factors obtained are given in Table VII. All the values for systems behaving normally

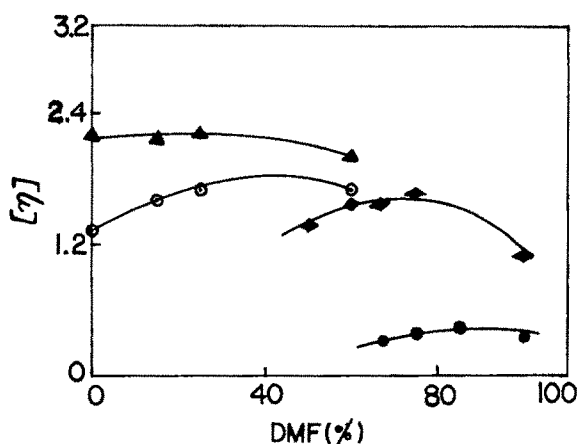


Figure 12 Plot of intrinsic viscosity $[\eta]$ versus percentage DMF for terpolymers (▲) I, (○) II, (■) III, (●) IV

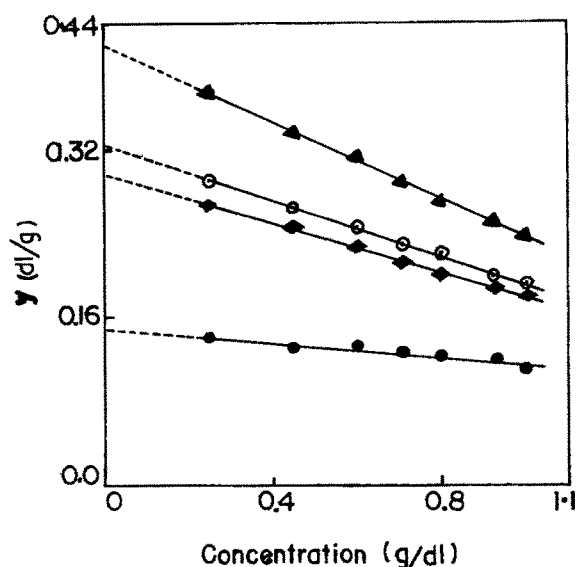


Figure 13 Plot of y versus concentration (C) for terpolymers (▲) I in water, (○) II in DMF H_2O (60/40), (■) III in DMF H_2O (50/50); (●) IV in DMF

(PAM in H_2O , PAN and set IV in DMF) were found to be around 2.5, indicating a spherical conformation³³ of the macromolecules in the solution. The ν values as shown in Table VII were found

to be independent of temperature (varying between 2.5 and 2.6), indicating that the minor axis varies by about 1%. The rest of the systems gave a higher value of ν due to both the complicated distribution in the solution of highly elongated chains and also because of their electrostatic interactions when highly charged. The change in the property of the polymer solution with a change in temperature depends on two antagonistic factors: (i) coiling/uncoiling of polymer chains and (ii) change in the degree of rotation about a skeletal bond.³⁴ The first one changes the length of the chain, and with increase in temperature, generally increases, leading to higher $[\eta]$ or higher ν . The second one increases the degree of rotation with increase in temperature and thereby should decrease $[\eta]$ and, hence, ν . From Table VII it can be seen that the shape factor ν , in general, somewhat decreases, that is, it is oblate spheroid³³ for almost all systems with increase in temperature, indicating a tendency toward spherical conformation at higher temperature.

The voluminosity V_E (dL/g) is a function of temperature and is a measure of the volume of solvated polymer molecules.³¹ As the temperature increases, desolvation takes place and, hence, V_E decreases. In our systems also, V_E values decrease

Table VII Voluminosity (V_E) and Shape Factor (ν) of Various Polymers at Different Temperatures

Polymer Systems/Solvent	30°C		35°C		40°C	
	V_E (dL/g)	ν	V_E (dL/g)	ν	V_E (dL/g)	ν
PAM/ H_2O	—	—	1.160	2.5	1.17	2.5
Set I/ H_2O	0.421	5.2	0.411	5.0	0.403	4.9
/85 : 15 H_2O : DMF	0.438	4.9	0.430	4.9	0.420	4.9
/75 : 25 "	0.428	5.2	0.424	5.0	0.421	5.0
/40 : 60 "	0.394	5.2	0.393	5.2	0.388	5.1
Set II/ H_2O	0.312	4.3	0.315	4.8	0.316	5.0
/85 : 15 H_2O : DMF	0.309	5.2	0.304	5.2	0.304	5.2
/75 : 25 "	0.314	5.5	0.313	5.2	0.311	5.0
/40 : 60 "	0.326	5.2	0.321	5.0	0.316	4.9
Set III/DMF	0.235	4.7	0.221	4.4	0.206	4.1
/50 : 50 H_2O : DMF	0.298	4.6	0.308	4.7	0.303	4.9
/40 : 60 "	0.320	4.9	0.316	4.8	0.314	4.8
/33 : 67 "	0.322	4.9	0.315	4.9	0.313	4.5
/25 : 75 "	0.325	5.2	0.321	4.8	0.314	4.6
Set IV/DMF	0.151	2.5	0.146	2.5	0.136	2.5
/33 : 67 H_2O : DMF	0.115	2.9	0.124	2.9	0.139	3.0
/25 : 75 "	0.135	3.0	0.128	2.7	0.126	2.5
/15 : 85 "	0.156	2.9	0.152	2.8	0.147	2.7
PAN/DMF	0.282	2.6	0.277	2.5	0.270	2.6

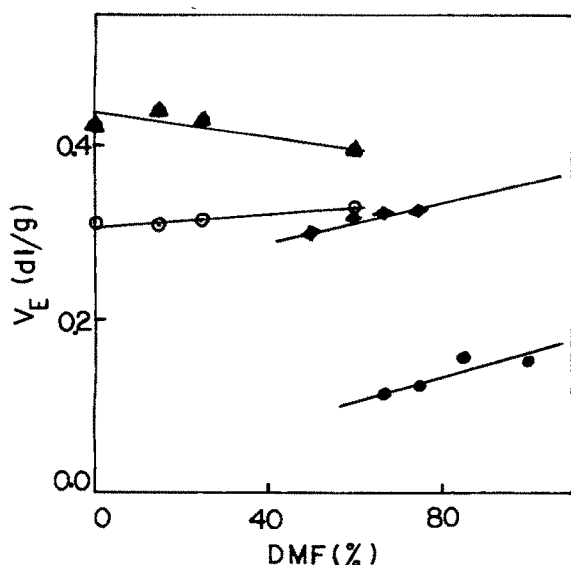


Figure 14 Plot of voluminosity (V_E) versus percent DMF for terpolymers. Symbols as in Figure 13.

with increase in temperature, indicating desolvation as shown in Table VII. For the highly water-soluble terpolymer of set I, the V_E decreases as the DMF concentration in the mixed solvent increases. For set II, which is partially water-soluble, V_E increases with increasing percent DMF composition. The same was observed for sets III and IV (Fig. 14). For set I which is water-soluble, the DMF : water mixture acts as a poor solvent because the V_E value decreases with increase in DMF concentrations. For other sets of polymers (II, III, and IV) which are partially water-soluble or -insoluble, the DMF : water mixture is a good solvent to a certain extent since V_E is found to increase with increasing DMF content.

CONCLUSION

On the basis of these results, it can be concluded that the free-radical terpolymerization reactions of acrylamide, acrylic acid, and acrylonitrile systems studied follow classic copolymerization theory. The higher reactivity of acrylamide than that of the other two monomers taken together were supported by the reactivity ratios. IR and ^1H -NMR spectroscopy provided evidence for the structure of the terpolymers and activation energies as well as the shape factors of the terpolymers that were obtained by TGA and solution viscosity studies.

The authors thank the Department of Biotechnology, Government of India, for financial assistance. They also thank the S P University, Vallabh Vidyanagar, for the elemental analysis.

REFERENCES

1. X. Jin, C. Carfagna, L. Nicolais, and R. Lanzetta, *Macromolecules*, **28**, 4785 (1995).
2. P. Shukla and A. K. Srivastava, *Polymer*, **35**, 4665 (1994).
3. P. Shukla and A. K. Srivastava, *Macromol. Rep., A*, **31**, 315 (1994).
4. A. A. Mahmoud, A. F. Shaaban, A. A. Khalil, and N. N. Massiha, *Polym. Int.*, **27**, 333 (1992).
5. G. Kysela and E. Staudner, *J. Polym. Mater.*, **9**, 297 (1992).
6. S. H. Ronel and D. H. Kohn, *J. Appl. Polym. Sci.*, **19**, 2359 (1975).
7. D. S. G. Hu and M. T. S. Lin, *Polymer*, **35**, 4416 (1994).
8. A. S. Teot, in *Encyclopedia of Chemical Technology*, Vol. 20, M. Grayson, Ed., Wiley, New York, 1980, p. 217.
9. J. D. Morris and R. J. Penzenstadler, in *Encyclopedia of Chemical Technology*, Vol. 10, M. Grayson, Ed., Wiley, New York, 1980, p. 321.
10. W. M. Thomas, in *Encyclopedia of Polymer Science and Technology*, Vol. 1, H. F. Mark, N. G. Gaylord, and N. M. Bikales, Eds., Wiley, New York, 1964, p. 181.
11. R. Joseph, S. Devi, and A. K. Rakshit, *J. Appl. Polym. Sci.*, **50**, 173 (1993).
12. A. Broido, *J. Polym. Sci.*, **7**, 1761 (1969).
13. F. Candau, Z. Zekhnini, F. Heatley, and E. Franta, *Colloid Polym. Sci.*, **264**, 676 (1986).
14. P. Bajaj, K. Sen, and S. Hajar Bahrami, *J. Appl. Polym. Sci.*, **59**, 1539 (1996).
15. T. Kelen and F. Tudos, *J. Makromol. Sci. Chem.*, **9**, 1 (1975).
16. M. Fineman and S. Ross, *J. Polym. Sci.*, **5**, 259 (1980).
17. N. A. Granem, N. A. Massiha, N. E. Ikladios, and A. F. Shaaban, *J. Appl. Polym. Sci.*, **26**, 97 (1981).
18. C. L. McCormick and G. S. Chen, *J. Polym. Sci.*, **22**, 3633, 3649 (1984).
19. C. L. McCormick and K. P. Blackmon, *Polymer*, **27**, 1971 (1986).
20. S. Igarshi, *J. Polym. Sci. Polym. Lett. Ed.*, **1**, 359 (1963).
21. D. H. Grand and N. Grassie, *Polymer*, **1**, 125 (1960).
22. L. M. Minsk, C. K. Chik, G. N. Meyer, and W. O. Kenyon, *J. Polym. Sci. Polym. Ed.*, **12**, 133 (1974).
23. M. Tutas, M. Saglam, M. Yuksel, and C. Guler, *Thermochim. Acta*, **111**, 121 (1987).
24. T. Ozawa, *J. Therm. Anal.*, **2**, 301 (1970).
25. T. Ozawa, *Bull. Chem. Soc. Jpn.*, **38**, 1881 (1965).

- 26 H Nishizaki, K Yoshida, and J H. Wang, *J Appl Polym Sci*, **25**, 2869 (1980)
- 27 V Vangani and A K Rakshit, *J Appl Polym Sci*, **45**, 1165 (1992)
- 28 R Joseph, S Devi, and A K Rakshit, *Polym Int*, **26**, 89 (1991)
- 29 T Ogawa and M. Sakai, *J Appl Polym Sci*, **23**, 2817 (1979)
- 30 P J Flory, *Principles of Polymer Chemistry*, 1st ed, Cornell University Press, New York, 1953, p 635
- 31 S Ajitkumar, D Prasadkumar, S Kansara, and N K Patel, *Eur Polym J*, **31**, 149 (1995)
- 32 H H Kohler and J Strand, *J Phys. Chem*, **94**, 7628 (1990)
- 33 G V. Vinogradov and A Ya. Malkin, *Rheology of Polymers*, Mir, Moscow, 1980
- 34 M Bhagat, S Joshi, S S Kansara, and N K Patel, *J Polym Mater*, **14**, 159 (1997)

Synthesis and Characterization Studies of Homopolymers of *N*-Vinylpyrrolidone, Vinyl Acetate, and Their Copolymers

ISMAIL MATHAKIYA, ANIMESH KUMAR RAKSHIT

Department of Chemistry, Faculty of Science, M S University of Baroda, Baroda 390 002, India

Received 26 April 1997, accepted 24 June 1997

ABSTRACT: Homopolymers of *N*-vinylpyrrolidone (VP) and vinyl acetate (VAc) were synthesized by a free-radical solution polymerization technique. Copolymers of VP and VAc in various monomer feed ratios were also synthesized by the same procedure. They were characterized by elemental analysis, FTIR, PNMR, TGA, swelling, and viscosity measurements. The reactivity ratios of the monomers were computed by both Fineman–Ross and Kelen–Tudos methods using data from both PNMR and elemental analysis studies. The activation energy values for various stages of decomposition were calculated from TGA analysis using Broido's method. The viscosity measurements were carried out at four different temperatures: 30, 35, 40, and 45°C. The activation parameters of the viscous flow, voluminosity (V_E), and shape factor (ν) were also computed for all systems. © 1998 John Wiley & Sons, Inc. *J Appl Polym Sci* 68: 91–102, 1998

Key words: TGA; PNMR, viscosity, homopolymer, copolymer, vinylpyrrolidone, vinyl acetate

INTRODUCTION

The synthesis of novel polymers with varied properties for different needs has been the focus of polymer research for many years. A wide variety of chemical or physical strategies including copolymerization, polymer blend formation, and crosslinking network formation have been explored to provide multifunctional polymers.¹ The accurate estimation of the composition of copolymers and the determination of monomer reactivity ratios are important for tailoring copolymers with the required physicochemical properties.² Copolymers and terpolymers containing *N*-vinylpyrrolidone (VP) find wide application in the field of hydrogels, pharmaceuticals, and cosmetics and in the food industry as well as in numerous other technical fields.³ It was decided, therefore, to co-

polymerize vinyl acetate (VAc) with VP since poly(vinyl acetate) (PVAc) is one of the most important of all the synthetic thermoplastic adhesives with wide range of industrial applications.⁴ The possibility of biodegradation of the P(VP–VAc) copolymer is also a major reason for the synthesis of these copolymers. In this article, we present the results of our study of the properties of PVP, PVAc, and their copolymers P(VP–VAc). Various studies, for example, IR, NMR, thermal degradation, swelling, and solution viscosity, were done. The results of these studies are discussed in this article.

EXPERIMENTAL

N-Vinylpyrrolidone (VP, Fluka) was used as received. Vinyl acetate (VAc, SD's Lab-Chem. Industry, Bombay, India) was vacuum-distilled and the middle fraction used for polymerization. Technical-grade azobisisobutyronitrile (AIBN) was recrystallized from warm methanol and stored at

Correspondence to: A. K. Rakshit
Contract grant sponsor: Department of Biotechnology, Government of India

Journal of Applied Polymer Science, Vol. 68, 91–102 (1998)
© 1998 John Wiley & Sons, Inc. CCC 0021-8995/98/010091-12

–20°C. The solvents, that is, benzene, *n*-hexane, *n*-heptane, *n*-octane, *n*-nonane, methanol, and chloroform, were obtained from Qualigens, India. All solvents were freshly distilled before use.

The FTIR of the films of the homopolymers and copolymers were recorded on a Bomem-MB104, Canada, FTIR spectrophotometer. The films were prepared by dissolving the polymers in chloroform and then pouring the solution over a pool of mercury. The films were obtained by vacuum evaporation of the solvent.

The NMR of the polymer solutions in CDCl₃ were recorded on a JEOL GSX, 400 MHz PMR at RSIC, IIT, Madras, India. The elemental analysis (viz., C and H) was carried out with a Coleman C, H analyzer and nitrogen was estimated by the Dumas method. TGA was recorded on a Shimadzu thermal analyzer DT-30B. The TGA analysis was done in the presence of air at three different heating rates, 10, 15, and 20 K min^{–1}.

The swelling behavior of the copolymers P(VP–VAc) with various compositions was studied on approximately uniform particle-size powdered samples. The swelling in different solvents was calculated using the following relation

$$S = \% \text{ swelling} = \frac{W - W_0}{W_0} \times 100$$

where *W* and *W*₀ are weights of the swollen and dry polymers, respectively.

Viscosity measurements of the dilute solution of the homopolymers and copolymers in chloroform were carried out using an Ubbelohde dilution viscometer suspended in a thermostated bath at the required temperature (±0.05°C). Measurements for each solution were repeated five to six times. Densities of the solutions at different temperatures were assumed to be those of solvents at that temperature.⁵ Polymerization of VP, VAc, and their copolymers, in various feed ratios, was carried out by the free-radical solution polymerization technique⁶ described below.

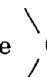
Polyvinylpyrrolidone (PVP) was synthesized as follows: Twenty percent (v/v) of VP in methanol and 0.2% (w/v) of AIBN as an initiator were taken in a three-necked flask under a nitrogen atmosphere. The reaction mixture was stirred at 75°C for a period of 7 h. The three-necked flask was equipped with a water condenser and was placed in a thermostat maintained at 75°C. The reaction mixture after polymerization was poured into an excess of *n*-hexane to precipitate out PVP

and then purified by repeated reprecipitations from the methanol solution into the *n*-hexane medium.

The synthesis of poly(vinyl acetate) (PVAc) was carried out in the following way: Ten grams of VAc in 20 mL of methanol was taken in a three-necked flask. The reaction setup was similar to that used for the synthesis of PVP. AIBN, 0.1 g, was used as the initiator. The reaction mixture was stirred for a period of 5 h, under a nitrogen atmosphere, at 65°C. PVAc was obtained by pouring the reaction mixture into nonsolvent water.

Copolymerization of VP and VAc was carried out with various different feed ratios, that is, 80 : 20, 60 : 40, 40 : 60, and 20 : 80 (v/v) of the two monomers.⁷ The recipe for the synthesis of a copolymer of 80 : 20 (v/v) of VP and VAc was as follows: 16 mL VP, 4 mL VAc, and 0.2 g AIBN were taken in 80 mL of benzene. The reaction was carried out under a nitrogen atmosphere at 70°C for a period of 10 h. The reaction setup of the PVP synthesis was used. The reaction mixture, after polymerization, was poured into an excess of *n*-hexane to precipitate out the product. The homopolymer PVP is insoluble in 2% acetone (v/v) in benzene although the copolymers are soluble. The precipitate was therefore treated with the above acetone–benzene solvent for 24 h with vigorous shaking. The residue was homopolymer PVP. The filtrate was then poured into an excess of *n*-hexane. The precipitated product was then Soxhlet-extracted with a toluene–cyclohexane mixture (80/20, v/v). The homopolymer PVAc is soluble in this mixture and, hence, was separated from the copolymer. The copolymer was washed well with cyclohexane and dried *in vacuo* before characterization.

FTIR spectroscopy is a powerful tool for structure elucidation.⁸ The position, intensity, and shape of vibrational bands are useful in clarifying conformational and environmental changes of polymers at the molecular level. It is well known^{9,10} that the infrared spectrum of PVAc exhibits changes with tacticity. The band at 1061 cm^{–1} is associated with the isotactic structure of the polymer [Fig. 1(a)]. The band at 617 cm^{–1} is very characteristic of PVAc due to the out-of-plane

CH₂–CO₂ bend. The  C=O band of PVAc was observed at 1734 cm^{–1}. Other prominent absorption peaks were at 1372 and 1431 cm^{–1}. These are due to the asymmetrical and symmetrical bending vibrations of C–CH₃. The asymmetric stretches

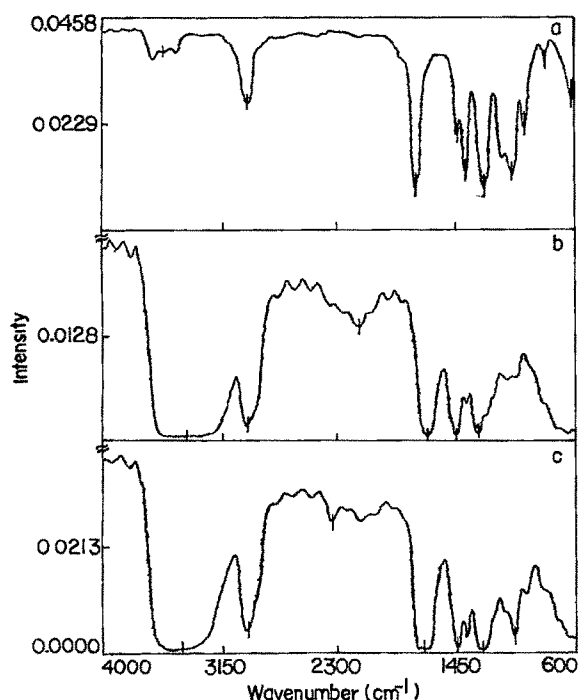


Figure 1 FTIR spectrum of (a) PVAc, (b) PVP, and (c) sample S2.

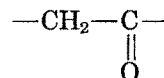
(C—O—C) were seen at 1245 cm^{-1} . Aliphatic stretches of C—H, due to $-\text{CH}_2$ and $-\text{CH}_3$, were also observed at 2951 cm^{-1} . These account for all the main absorption bands of PVAc. The assignments were done with the help of the literature data.¹¹

The FTIR of PVP showed characteristic absorptions which agreed very well with those reported in the literature³ and are given in Figure 1(b). The strong absorption at 1654 cm^{-1} is associated with the $\text{C}=\text{O}$ absorption of tertiary amide and

of the five-membered ring. This $\text{C}=\text{O}$ band oc-

curs at a longer wavelength than normal carbonyl absorption due to the resonance effect. The C—N stretching absorption appears at 1283 cm^{-1} . This is at higher frequency than the corresponding absorption of normal aliphatic amine because the force constant of the C—N bond is increased by

resonance with the ring $\text{C}=\text{O}$ groups. The scissoring band (δ , CH_2) in the spectra was observed at 1445 cm^{-1} due to the



(small ring) and $-\text{CH}_2-\text{N}$ (amides) groups

of PVP. Besides this, the asymmetrical stretching ($\nu_{\text{as}}\text{CH}_2$) occurs near 2934 cm^{-1} .

Figure 1(c) shows the FTIR of the P(VP-VAc) copolymer (S2). It is similar to the FTIR of PVP [Fig. 1(b)]. The VAc group incorporated could not be very well distinguished by FTIR, but was supported by PNMR spectroscopy as shown below.

The evidence for the two monomers being incorporated was given by the PNMR spectra of the copolymers.^{2,3,10-12} The signals appropriate to this discussion are represented in Figure 2 as (a–c), corresponding to protons on the VAc in the copolymer, and signals (d–h) corresponding to protons on the VP moiety in the copolymer. In the PNMR spectrum of the copolymer (S1, VP = 59.5 mol % in the copolymer, Fig. 3), the signals that occur around $\delta = 4.77\text{ ppm}$ (ref. 12) are associated with the methine backbone protons (b), whereas methine backbone protons (e) appear as a broad peak at $\delta = 3.75\text{--}3.95\text{ ppm}$.^{2,3} It was shown that the three peaks of the acetoxy proton signals [3H, (c) in Fig. 2] and methylene backbone protons (d) resonate at 1.98, 2.00, and 2.02 ppm.¹⁰ Various resonances in this area cannot be distinguished because of the overlap due to spin–spin coupling and the sensitivity of methyl protons toward tacticity and the monomer sequence.¹² Besides this, one can see from Figure 3 that signals from protons (a) and (g) overlap and give a broad peak at around 1.427–1.695 ppm, whereas protons (f) resonate at around $\delta = 3.08\text{--}3.42\text{ ppm}$.¹¹

The change in the composition of the copolymer of VP (1) on the copolymerization with VAc (2) is expressed by the following relations:

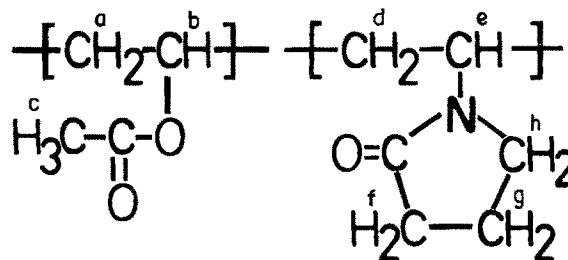


Figure 2 Repeat unit in the homopolymers and/or copolymers

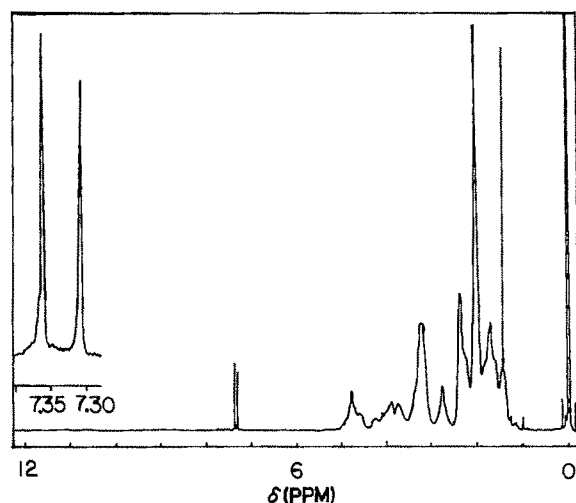


Figure 3 PNMR spectrum of the copolymer S1 (VP = 59.5 mol % in the copolymer) in CDCl_3

$$\frac{\phi_1}{\phi_2} = \frac{r_1 M_1^2 + M_1 M_2}{r_2 M_2^2 + M_1 M_2} \quad (1)$$

The above equation can be rewritten as¹³

$$r_2 = r_1 H^2/h + H(1-h)/h \quad (2)$$

where $H = M_1/M_2$ and $h = \phi_1/\phi_2$. M_1 and M_2 are mole fractions of the monomers in the feed, and

ϕ_1 and ϕ_2 are the mole fractions of the monomers in the relevant copolymer (as defined in Tables I and II). r_1 and r_2 are the reactivity ratios of the two monomers. The mole fractions of the monomers in the copolymers were determined from the PNMR spectral data.

The mole fraction of VP (ϕ_1) in the copolymer was determined using the following relation:

$$\phi_1 = \frac{I(-\text{CH of VP})}{I(-\text{CH of VAc}) + I(-\text{CH of VP})} \quad (3)$$

where $I(-\text{CH of VP})$ and $I(-\text{CH of VAc})$ represent the peak intensities of the $-\text{CH}$ protons of VP and VAc, respectively. The $-\text{CH}$ proton of VP resonates at 3.75–3.95 ppm, whereas the $-\text{CH}$ proton of VAc resonates at 4.77 ppm. The mole fractions of VP and VAc in the copolymers of various compositions calculated by using PNMR are listed in Table I.

Monomer reactivity ratios r_1 and r_2 could thus be calculated graphically by plotting $H(1-h)/h$ versus H^2/h [Fineman–Ross (F–R) method]. The slope and intercept yielded r_1 (=0.174) and r_2 (=0.137) for VP and VAc (Table III), respectively.¹⁴

Reactivity ratios were also determined using the Kelen–Tudos (K–T) methods.¹⁵ Equation (1) can be rewritten as

Table I Composition of VP (1) and VAc (2) in the Feed and in the Copolymers

Polymer Samples	Mole Fraction (M) of VP and VAc in Feed		Elemental Analysis Data			Mole Fraction ^b (m) of VP and VAc in Copolymer		Mole Fraction ^c (ϕ) of VP and VAc in Copolymer	
	M_1	M_2	Nitrogen ^a (wt %)	Carbon (wt %)	Hydrogen (wt %)	m_1	m_2	ϕ_1	ϕ_2
S1 {NVP–VAc 80 20}	0.756	0.244	8.28	56.90	7.89	0.598	0.402	0.595	0.405
S2 {NVP VAc 60 40}	0.537	0.463	7.35	56.97	7.77	0.520	0.480	0.528	0.472
S3 {NVP VAc 40 60}	0.341	0.659	6.62	57.52	7.47	0.462	0.538	0.469	0.531
S4 {NVP VAc 20 80}	0.162	0.838	4.88	57.54	7.45	0.329	0.671	0.341	0.659
PVP	—	—	11.23	55.51	8.29	—	—	—	—
PVAc	—	—	—	55.28	6.96	—	—	—	—

^a Average of two pairs of duplicate analysis on each preparation

^b Calculated using elemental analysis data

^c Calculated using PNMR spectroscopic data

Table II K-T Parameters for the Monomer VP and VAc Using PNMR Spectroscopic Data

Polymer Samples	$H = \frac{M_1}{M_2}$	$h = \frac{\phi_1}{\phi_2}$	$G = \frac{H(h-1)}{h}$	$F = \frac{H^2}{h}$	$\beta = \frac{G}{\alpha + F}$	$\varepsilon = \frac{F}{\alpha + F}$
S1	3.10	1.47	0.99	6.53	0.90	0.14
S2	1.16	1.12	0.12	1.20	—	—
S3	0.52	0.88	-0.07	0.30	0.31	-0.07
S4	0.19	0.52	-0.18	0.07	0.09	-0.24

$\alpha = \sqrt{F_{\max} F_{\min}} = 0.68$ M_1 is the mole fraction of VP and M_2 is the mole fraction of VAc in the feed ϕ_1 and ϕ_2 are their respective experimental mole fractions in the copolymer, obtained from PNMR spectroscopic data

$$G/(\alpha + F) = (r_1 + r_2/\alpha)F/(\alpha + F) - r_2/\alpha \quad (4)$$

where G , F , and α are mathematical functions of H and h as defined in Table II. On plotting $G/(\alpha + F)$ as a function of $F/(\alpha + F)$, a straight line was obtained. This, when extrapolated to $F/(\alpha + F) = 0$ and $F/(\alpha + F) = 1$, gave $-r_2/\alpha$ and r_1 (both as intercepts), respectively. r_1 and r_2 were found to be 0.189 and 0.169 for VP and VAc, respectively (Table III). The calculated values were found to differ from the literature values^{16,17} (Table III). The values, particularly of ref. 17, are far from the values obtained by us. We are not in a position to explain these discrepancies.

The experimental feed ratios of the various monomers as well as the composition of the resulting copolymers, obtained by elemental analysis, are also summarized in Table I. The reactivity ratios (r) of VP and VAc in the copolymer were also determined by the F-R method¹⁸ using elemental analysis data. The following equation was used:

$$X(Y - 1)/Y = r_1 X^2/Y - r_2 \quad (5)$$

where $X = M_1/M_2$ and $Y = m_1/m_2$ (as defined in Table I).

On plotting $X(Y - 1)/Y$ against X^2/Y , a straight line was obtained, whose slope was r_1 and inter-

cept yielded r_2 . The values obtained for r_1 and r_2 are 0.184 and 0.168, respectively (Table III).

The reactivity ratios r_1 and r_2 of VP and VAc, respectively, in the copolymers were also estimated by the method of K-T:

$$\beta = r_1\varepsilon - r_2(1 - \varepsilon)/\alpha \quad (6)$$

where β , ε , and α are mathematical functions of G and F as defined in Table IV. The β versus ε plot was linear (Fig. 4) and r_1 and r_2 were found to be 0.182 and 0.142, respectively, for VP and VAc. The $r_1 r_2$ values (Table III) indicate that the copolymers should have a random distribution of the monomer units with a tendency toward alternation.¹⁹ It is to be noted that the estimated nitrogen in PVP is somewhat lower (Table I) than the expected value of 12.6%. Our repeated determination on fresh samples did not improve the value. However, this discrepancy in the estimated nitrogen value was also reported earlier.^{17,20,21} The compositions of the copolymers were computed by assuming a theoretical nitrogen value of 12.6% in PVP. The copolymer compositions computed from the nitrogen estimation as well as from PNMR are almost the same, indicating that the nitrogen estimated in the copolymers is probably correct. Why there has always been error in the estimation of nitrogen in PVP is not understood, although high hygroscopicity may be the reason.²¹

Table III Monomer Reactivity Ratios for Copolymerization of VP with VAc

Monomer	By Elemental Analysis		By PNMR Spectroscopy		Ref. 16	Ref. 17
	F-R Methods	K-T Methods	F-R Methods	K-T Methods		
VP (r_1)	0.184	0.182	0.174	0.189	0.44	2.28
VAc (r_2)	0.168	0.142	0.137	0.169	0.38	0.24
$r_1 r_2$	0.031	0.026	0.024	0.032	—	—

Table IV K-T Parameters for the Monomer VP and VAc Using Elemental Analysis Data

Polymer Samples	$X = \frac{M_1}{M_2}$	$Y = \frac{m_1}{m_2}$	$G = \frac{X(Y-1)}{Y}$	$F = \frac{X^2}{Y}$	$\beta = \frac{G}{\alpha + F}$	$\varepsilon = \frac{F}{\alpha + F}$
S1	3.10	1.49	1.02	6.45	0.14	0.90
S2	1.16	1.08	0.09	1.24	0.05	0.64
S3	0.52	0.86	-0.09	0.31	-0.09	0.31
S4	0.19	0.49	-0.20	0.08	—	—

$\alpha = \sqrt{F_{\max} F_{\min}} = 0.70$ M_1 is the mole fraction of VP and M_2 is the mole fraction of VAc in the feed m_1 and m_2 are their respective experimental mole fractions in the copolymer, obtained from elemental analysis data

Further, as both r_1 and r_2 values are almost same, we can conclude that the composition of the copolymer does not vary with time and, therefore, the equations used to compute the reactivity ratios are justified. The low $r_1 r_2$ values (~ 0.03) indicate that the copolymer is more an alternating copolymer rather than a completely random copolymer.

The statistical distributions of the monomer sequence, 1-1, 2-2, and 1-2, were calculated using the following relations²²⁻²⁴:

$$X' = \phi_1 - 2\phi_1\phi_2 / \{1 + [(2\phi_1 - 1)^2 + 4r_1r_2\phi_1\phi_2]^{1/2}\} \quad (7)$$

$$Y' = \phi_2 - 2\phi_1\phi_2 / \{1 + [(2\phi_1 - 1)^2 + 4r_1r_2\phi_1\phi_2]^{1/2}\} \quad (8)$$

$$Z' = 4\phi_1\phi_2 / \{1 + [(2\phi_1 - 1)^2 + 4r_1r_2\phi_1\phi_2]^{1/2}\} \quad (9)$$

where r_1 and r_2 are the reactivity ratios of VP and VAc, respectively. ϕ_1 and ϕ_2 are the mole fractions of VP and VAc in the copolymer, obtained from the PNMR spectroscopic technique. The mole fractions of the 1-1, 2-2, and 1-2 sequences, that is, the blockiness, are designated by X' , Y' , and Z' , respectively (Table V). The mean sequence lengths μ_1 and μ_2 were calculated utilizing the relations

$$\mu_1 = 1 + r_1(\phi_1/\phi_2) \quad (10)$$

$$\mu_2 = 1 + r_2(\phi_2/\phi_1) \quad (11)$$

where the r_1 and r_2 values used were from Table III (K-T method).

The intermonomer linkages and mean sequence length distributions for the P(VP-VAc) copolymers are listed in Table V. For the series of P(VP-VAc) copolymers, μ_1 varied from 2.278 to 1.098 as the mole ratio of VP/VAc decreased. The calculated mole fraction of 1-2 linkages obtained in each copolymer was relatively high, indicating an alternating tendency of the copolymer formation, which was also concluded from the reasonably low values (~ 0.03) of $r_1 r_2$.

The thermogravimetric analysis (TGA) was done to study the thermal decomposition of polymers and also to determine the activation energy for decomposition. TGA curves of PVP, PVAc, and a copolymer (S3) are given in Figure 5. The thermogram of the copolymer (S3) falls in between those of the homopolymers, indicating a somewhat intermediate thermal stability. Other copolymers also show intermediate thermal stabil-

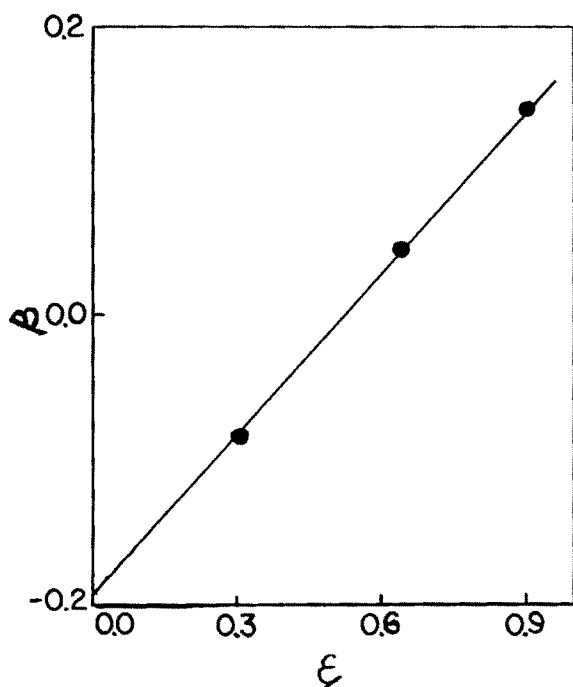


Figure 4 K-T plot for copolymerization of VP with VAc.

Table V Structural Data for the Copolymers of VP (1) with VAc (2)

Polymer Samples	Composition ^a (Mole Fraction)		Blockiness ^b (Mole Fraction)		Alternation ^b (Mole Fraction) 1-2 (Z')	Mean Sequence Length		$\frac{\mu_1}{\mu_2}$
	ϕ_1	ϕ_2	1-1 (X')	2-2 (Y')		μ_1	μ_2	
S1	0.595	0.405	0.212	0.022	0.766	2.278	1.115	2.043
S2	0.528	0.472	0.108	0.052	0.840	2.211	1.151	1.921
S3	0.469	0.531	0.050	0.112	0.838	1.167	1.191	0.980
S4	0.341	0.569	0.010	0.329	0.661	1.098	1.327	0.827

^a From PNMR spectra^b Statistically calculated using reactivity ratios

ity. Two-stage decomposition was observed in all cases, except for PVAc, which showed one-stage decomposition. The activation energy associated with each stage of decomposition was evaluated by the well-known Broido method^{25,26}. The equation used for the calculation of the activation energy (E_a) was

$$\ln \ln(1/Y'') = (-E/R)(1/T) + \text{constant} \quad (12)$$

where

$$Y'' = (W_t - W_\infty)/(W_0 - W_\infty) \quad (13)$$

that is, Y'' is the fraction of the number of initial molecules not yet decomposed; W_t , the weight at any time " t "; W_∞ , the weight at infinite time (= zero), and W_0 , the initial weight.

A plot of $\ln \ln(1/Y'')$ versus $(1/T)$ [eq (12)] gives an excellent approximation to a straight line over a range of $0.999 > Y'' > 0.001$. The slope is related to the activation energy. Representative plots are shown in Figure 6. The values for the activation energy of decomposition were evaluated at three different heating rates of 10, 15, and 20°C/min in air and are listed in Table VI.

The swelling is a measure of interaction be-

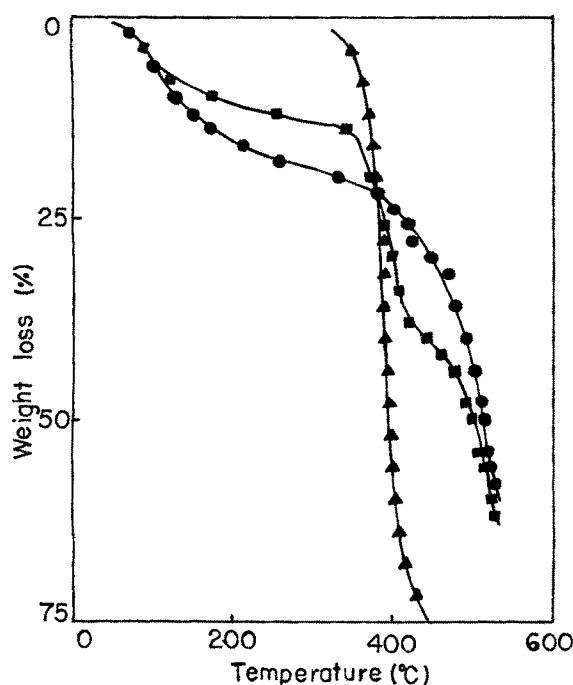


Figure 5 Representative TGA plots of (▲) PVAc, (●) PVP, and (■) copolymer S3 at heating rate of 10 K min⁻¹ in air

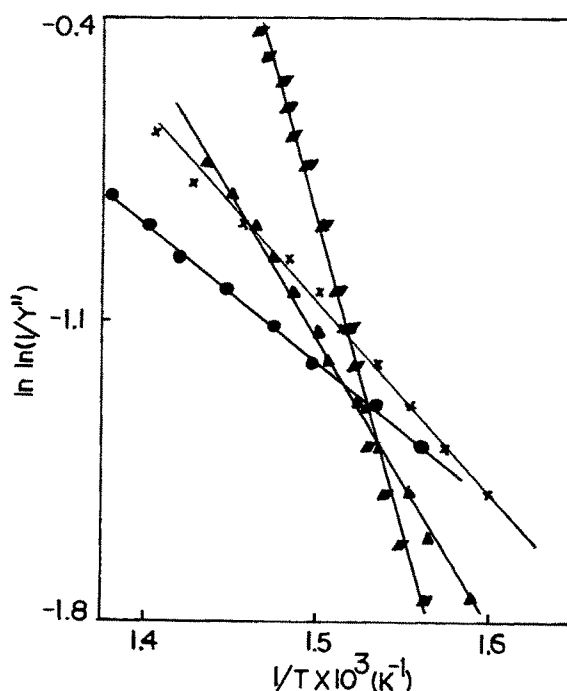


Figure 6 Activation energy plot for the copolymers (●) S1, (×) S2, (▲) S3, (■) S4

Table VI Activation Energy (E_a) of Decomposition for Various Homopolymers and Copolymers in Different Ratios by Thermogravimetric Analysis

Polymer Samples	Decomposition Temperature ^a Range (°C)	Weight Loss (%) ^a	E_a^b (kJ mol ⁻¹)		
			10°C min ⁻¹	15°C min ⁻¹	20°C min ⁻¹
PVP	103–380	22	6.2	13.7	6.8
	400–523	56	59.6	33.2	24.8
S1	68–153	14	40.7	36.3	15.7
	368–525	52	27.5	33.1	36.4
S2	68–139	12	34.5	15.0	34.3
	335–513	62	31.4	32.9	34.1
S3	70–123	08	38.7	34.7	11.9
	356–526	62	36.1	61.9	91.5
S4	39–336	08	6.6	26.0	8.9
	352–414	50	109.8	118.4	125.9
PVAc	351–416	68	203.2	234.5	259.8

^a Heating rate, 10°C min⁻¹

^b Calculated using the Brodov method at a heating rates of 10, 15, and 20°C min⁻¹ in air

tween polymer chains and the solvent molecule. It is a process of sorption/diffusion of a low molecular weight solvent by/in a polymer but it is accompanied by a change in the polymer structure. The penetration of a solvent into the interstructural space of a polymer causes the super-molecular structures of polymers to expand.^{9,27} The swelling data of P(VP-VAc) copolymers, as uncrosslinked, linear, and semicrystalline polymers in various hydrocarbons as solvents, are shown in Figure 7. It is observed that the percent swelling increases with increase of the VAc content in the copolymer up to around a 0.7 mole fraction before its decrease in all solvents. In Table VII, we present the densities of all copolymers. The notable point is that as the concentration of VAc in the copolymer increases the density decreases up to about a 0.7 mole fraction. In other words, the polymer structure becomes highly porous with increasing VAc. Thus, in turn, accepts more solvent and, hence, higher swelling. With further increase in the VAc concentration, the copolymer structure becomes more condensed and, hence, there is less swelling. The swelling coefficient also shows the same trend, which was calculated using the following equation⁹.

$$Q = \frac{W - W_0}{W_0} \frac{1}{d} \quad (14)$$

where Q is the swelling coefficient; W , the weight of the swollen polymer; W_0 , the initial weight of the polymer prior to swelling, and d , the density of the solvent used. The values obtained for the swelling and the swelling coefficient are shown in Table VII. All measurements were in duplicate.

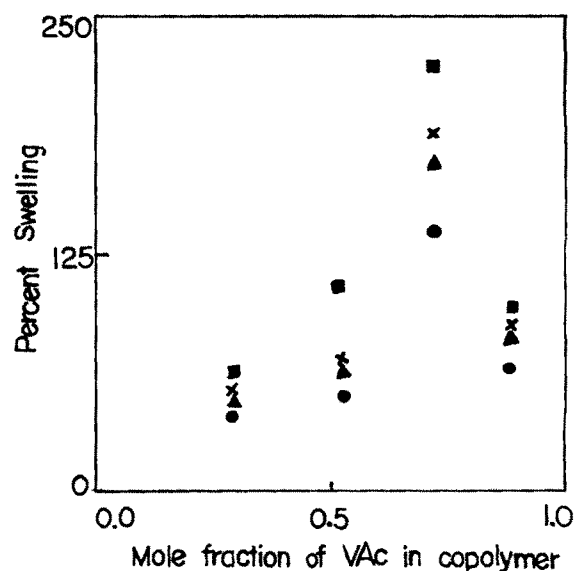


Figure 7 Swelling behavior of copolymers in solvents: (●) *n*-hexane, (▲) *n*-heptane, (×) *n*-octane; (■) *n*-nonane

Table VII Swelling Measurements of P (VP-VAc) Copolymers Using Different Solvents at Room Temperature

Polymer Samples	Swelling Time (h)	Density of the Polymer ρ (g/mL)	Solvent Used							
			<i>n</i> -Hexane		<i>n</i> -Heptane		<i>n</i> -Octane		<i>n</i> -Nonane	
			S^a	Q^b	S^a	Q^b	S^a	Q^b	S^a	Q^b
S1	25	0.9790	41.6	0.6313	49.0	0.6979	56.7	0.8284	67.5	0.9398
S2	25	0.9581	52.0	0.7891	63.4	0.9018	69.8	1.0211	129.8	1.8078
S3	25	0.9103	139.3	2.1138	173.8	2.4723	190.1	2.7797	226.0	3.1476
S4	25	0.9881	67.5	1.0240	82.2	1.1693	84.4	1.2345	84.3	1.3131

^a Percent swelling^b Swelling coefficient

In Table VIII, the intrinsic viscosities $[\eta]$ of all systems at various temperatures are given. They were computed by the well-known procedure.²⁸ The accuracy of the data was checked by calculating K' and K'' , and their differences were 0.5, as expected (Fig. 8).²⁹ The correlation coefficient was always 0.99 or better. It can be seen that $[\eta]$ decreases as the temperature increases and $[\eta]$ versus T plots were always linear with a negative slope. This result is because a temperature increase may lower the rotational barrier, thereby enhancing the degree of rotation about a skeletal bond, forcing the molecular chains to assume a more compact coiled configuration.

The viscosities of the polymer solutions were determined at different temperatures. The well-known Frenkel-Eyring equation

$$\eta = \frac{Nh}{V} \exp(\Delta G_{\text{vis}}^\ddagger / RT) \quad (15)$$

was used to evaluate various activation parameters of the viscous flow³⁰ and where V is the molar

volume of the solution; N , Avogadro's number; h , Planck's constant; R , the gas constant, T , the temperature; and $\Delta G_{\text{vis}}^\ddagger$, the activation free-energy change of the viscous flow. The above equation can be rewritten as

$$\begin{aligned} \ln(\eta V / Nh) &= \Delta G_{\text{vis}}^\ddagger / RT \\ &= \Delta H_{\text{vis}}^\ddagger / RT - \Delta S_{\text{vis}}^\ddagger / R \quad (16) \end{aligned}$$

where $\Delta H_{\text{vis}}^\ddagger$ and $\Delta S_{\text{vis}}^\ddagger$ are the activation enthalpy and the entropy change for the viscous flow, respectively. V is the molar volume of the

Table VIII Intrinsic Viscosities of Various Copolymers and the Homopolymers at Different Temperatures in Chloroform

Polymer Samples	$[\eta]$ (dL g ⁻¹)				$K' - K''$ (35°C)
	30°C	35°C	40°C	45°C	
PVP	0.368	0.366	0.363	0.358	0.51
S1	0.316	0.310	0.301	0.294	0.51
S2	0.318	0.314	0.310	0.308	0.51
S3	0.305	0.299	0.294	0.288	0.50
S4	0.290	0.276	0.269	0.266	0.51
PVAc	0.632	0.614	0.612	0.608	0.49

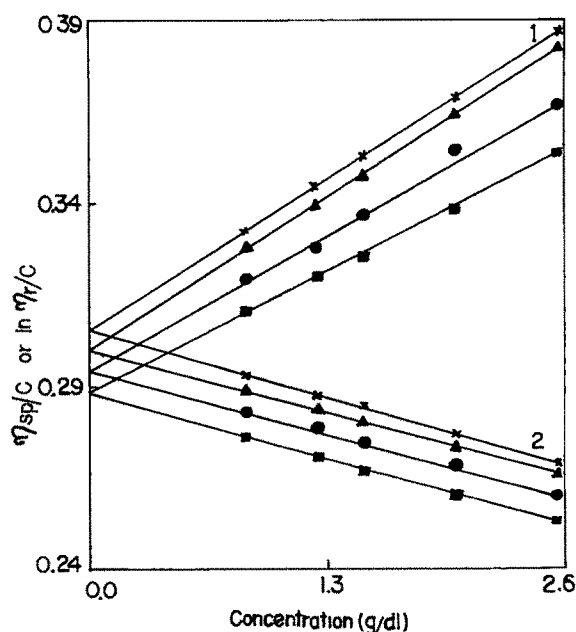


Figure 8 Typical plot of (1) η_{sp}/c and (2) $\ln \eta_r/c$ against concentration for copolymer S3: (x) 30°C, (Δ) 35°C, (●) 40°C; (■) 45°C

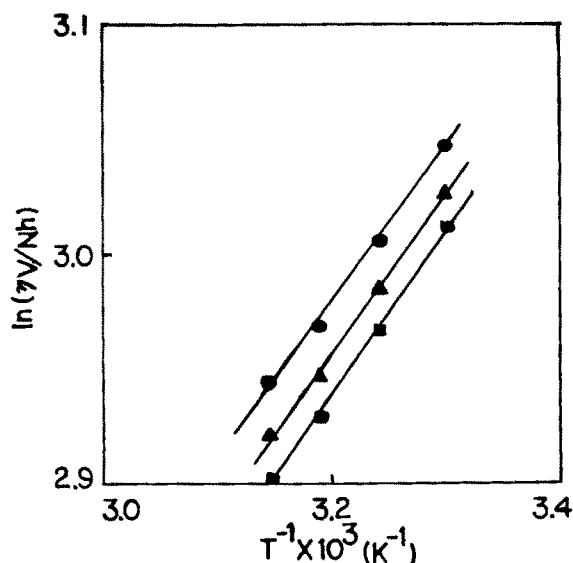


Figure 9 Plots of $\ln(\eta V/Nh)$ against $1/T$ for 0.5 g dL solutions in CHCl_3 (●) PVP, (▲) S2, (■) S4

solution and was taken as equal to the molar volume of the solvent.³¹ The plot of $\ln(\eta V/Nh)$ against T^{-1} shows linearity with correlation coefficients of 0.99 or better for all systems (Fig. 9). The slope and intercept gave $\Delta H_{\text{vis}}^\ddagger$ and $\Delta S_{\text{vis}}^\ddagger$, respectively. The calculated values of $\Delta G_{\text{vis}}^\ddagger$, $\Delta H_{\text{vis}}^\ddagger$, and $\Delta S_{\text{vis}}^\ddagger$ for some representative systems at a concentration of 0.5 g dL⁻¹ are listed in Table IX. The $\Delta H_{\text{vis}}^\ddagger$ and $\Delta S_{\text{vis}}^\ddagger$ for all systems are constant quantities, independent of temperature, which signifies that the systems are not cross-linked. It is also observed that the heats of activation of viscous flow are positive (Table IX). The values are not large. The highest value observed was around 6.10 kJ mol⁻¹ for S4 at a 0.5 g dL⁻¹ concentration. The entropies of activation of the

viscous flow are also low and negative, indicating that the polymer structures are poorly ordered in chloroform. The $\Delta H_{\text{vis}}^\ddagger$ and $\Delta S_{\text{vis}}^\ddagger$ of this system seem to be almost same for all copolymers and both homopolymers with an average value of 5.9 ± 0.1 kJ mol⁻¹ and -6.0 ± 0.3 J mol⁻¹ K⁻¹, respectively. This constancy indicates that the structures of the solutions are similar in all respects. The $\Delta G_{\text{vis}}^\ddagger$ at all temperatures can, hence, be calculated.

Relative viscosity data at different concentrations were also used to calculate the voluminosity, V_E , of the polymer solutions at different temperatures in chloroform (Table X). V_E was calculated by plotting ψ against the concentration (in g dL⁻¹), where

$$\psi = (\eta_r^{0.5} - 1)/C(1.35\eta_r^{0.5} - 0.1) \quad (17)$$

The straight line obtained was then extrapolated to $C=0$ and the intercept yielded V_E (Fig. 10). The shape factor was obtained from the equation^{27,31-33}

$$[\eta] = \nu V_E \quad (18)$$

The shape factor gives an idea about the shape of the polymer molecules in solution.³⁴ The shape factors in different temperatures were found to be 2.5 ± 0.2 , suggesting that the macromolecules acquire a spherical conformation.³⁵ Moreover, the ν values were found to be independent of temperature, suggesting that the conformation was not dependent on temperature. The voluminosity (Table X) is a function of temperature. V_E is a measure of volume of solvated polymer molecules.³⁶ As the temperature increases, desolvation takes place and, hence, V_E decreases. In our systems,

Table IX Free Energy $\Delta G_{\text{vis}}^\ddagger$, Enthalpy $\Delta H_{\text{vis}}^\ddagger$, and Entropy $\Delta S_{\text{vis}}^\ddagger$ of Activation for Viscous Flow of the P (VP-VAc) Copolymers and Respective Homopolymers in Chloroform

Polymer Samples	$\Delta G_{\text{vis}}^\ddagger$ (kJ mol ⁻¹)				$\Delta H_{\text{vis}}^\ddagger$ (kJ mol ⁻¹)	$\Delta S_{\text{vis}}^\ddagger$ (J mol ⁻¹ K ⁻¹)
	30°C	35°C	40°C	45°C		
PVP	7.66	7.70	7.73	7.76	5.69	-6.51
S1	7.61	7.64	7.67	7.70	5.78	-6.03
S2	7.62	7.65	7.68	7.71	5.72	-6.26
S3	7.59	7.62	7.65	7.68	5.83	-5.82
S4	7.58	7.61	7.63	7.65	6.10	-4.89
PVAc	7.98	8.01	8.04	8.08	5.97	-6.62

Concentration of the solution was 0.5 g dL⁻¹

Table X Hydrodynamic Volumes (V_E) and Shape Factor (ν) of Various Polymers at Different Temperatures

Polymer Samples	30°C		35°C		40°C		45°C	
	V_E (dL g ⁻¹)	ν	V_E (dL g ⁻¹)	ν	V_E (dL g ⁻¹)	ν	V_E (dL g ⁻¹)	ν
PVP	0.145	2.6	0.144	2.5	0.141	2.6	0.140	2.5
S1	0.121	2.6	0.120	2.5	0.118	2.5	0.116	2.5
S2	0.122	2.6	0.121	2.5	0.121	2.5	0.121	2.5
S3	0.118	2.5	0.117	2.5	0.114	2.5	0.114	2.5
S4	0.112	2.6	0.108	2.5	0.106	2.6	0.105	2.5
PVAc	0.232	2.7	0.227	2.7	0.230	2.6	0.288	2.6

the V_E also decreases with increase in temperature, indicating desolvation (Table X). The biodegradative nature of these copolymers is presently being tested.

CONCLUSIONS

On the basis of the above-mentioned results, it can be concluded that the free-radical copolymerization reaction of VP with VAc systems studied follows the classical copolymerization theory. FTIR and PNMR spectroscopy provided evidence for the structure of the copolymers. The reactivity ratios of the monomers were obtained by both ele-

mental analysis and PNMR spectroscopy and did show relatively higher reactivity of VP than of VAc. The monomer units in the copolymer show a tendency toward alternation and the composition of the copolymer does not seem to vary with time. The activation energy of decomposition, viscosity activation parameters, and shape factors were obtained by TGA and solution viscosity studies. The viscosity activation parameters indicate that the polymers in chloroform solutions are not crosslinked and the structure of homopolymer and copolymer solutions are similar.

Thanks are due to the Department of Biotechnology, Government of India, for financial assistance. Thanks are also due to Dr. C. F. Desai for the FTIR studies.

REFERENCES

1. X. Jin, C. Carfagna, L. Nicolais, and R. Lanzetta, *Macromolecules*, **28**, 4785 (1995).
2. T. Narasimhaswamy, B. S. R. Reddy, S. C. Sumathi, and S. Rajadurai, *J. Polym. Mater.*, **6**, 209 (1989).
3. F. Haaf, A. Sanner, and F. Straub, *Polym. J.*, **17**, 143 (1985).
4. C. D. Han, Y.-J. Ma, and S. G. Chu, *J. Appl. Polym. Sci.*, **32**, 5597 (1986).
5. H. Tompa, *Polymer Solutions*, Butterworth, London, 1956, p. 287.
6. K. Noro, in *Poly Vinyl Alcohol. Properties and Applications*, C. A. Finch, Ed., Wiley-Interscience, New York, 1973, p. 68.
7. D. H. Lorenz, in *Encyclopedia of Polymer Science and Technology*, Vol. 14, H. F. Mark, N. G. Gaylord, and N. M. Bikales, Eds., Wiley, New York, 1964, p. 241.
8. W. K. Lee and C. S. Ha, *Polymer (Korea)*, **18**, 935 (1994), *Chem. Abstr.*, **122**, 56997k (1995).

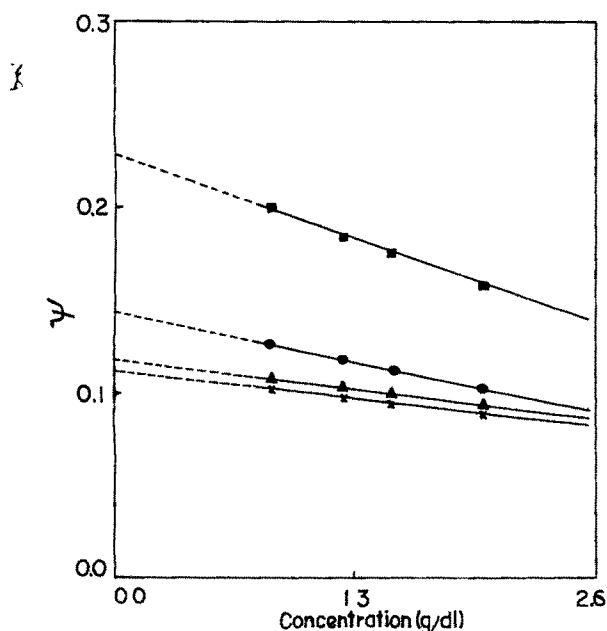


Figure 10 Plot of ψ versus concentration for polymers (■) PVAc, (●) PVP, (▲) S3, (×) S4

- 9 S K Verma, P. Arvindakshan, and S C Bisarya, *J Appl Polym Sci*, **46**, 707 (1992)
- 10 M K Lindemann, in *Encyclopedia of Polymer Science and Technology*, Vol. 15, H. F Mark, N G Gaylord, and N M Bikales, Eds., Wiley, New York, 1964, pp 546, 549
- 11 R M Silverstien, R G Bessler, and T C Morrill, *Spectroscopic Identification of Organic Compounds*, 4th ed Wiley, New York, 1981
- 12 A S Brar and S Charan, *J Appl Polym Sci*, **53**, 1813 (1994)
- 13 V. Vangani and A. K. Rakshit, *J Appl. Polym Sci*, **60**, 1005 (1996)
- 14 I K Varma, M V Nair, and V. K. Karan, *J Therm Anal*, **35**, 989 (1989)
- 15 T Kelen and F Tudos, *J Macromol Sci Chem.*, **9**, 1 (1975)
- 16 K Hayashi and G Smets, *J Polym Sci*, **27**, 275 (1958)
- 17 D. J Khan and H H. Horowitz, *J Polym Sci.*, **54**, 363 (1961)
- 18 M. Fineman and S. Ross, *J Polym Sci.*, **5**, 259 (1980)
- 19 N A Granem, N A Massiha, N E Ikladious, and A F Shaaban, *J Appl Polym Sci*, **26**, 97 (1981)
- 20 M. A Al-Issa, T P Davis, M B Huglin, and D C F Yip, *Polymer*, **26**, 1869 (1985)
- 21 S Wen, Y Xiaonan, and W T K Stevenson, *Polym. Int.*, **27**, 81 (1992)
- 22 C L McCormick and G S Chen, *J Polym Sci.*, **22**, 3633, 3649 (1984)
- 23 C L McCormick and K P Blackmon, *Polymer*, **27**, 1971 (1986)
- 24 S Igarshi, *J Polym. Sci Polym Lett Ed*, **1**, 359 (1963)
- 25 A. Broido, *J Polym Sci*, **7**, 1761 (1969)
- 26 R Joseph, S Devi, and A K Rakshit, *J Appl Polym Sci*, **50**, 173 (1993)
- 27 A K. M. Asaduzzaman, A K Rakshit, and S Devi, *J Appl. Polym Sci*, **47**, 1813 (1993)
- 28 A Tager, *Physical Chemistry of Polymers*, Mir, Moscow, 1978, p 456
- 29 E A Collins, J Bares, and F W Billmeyer, *Experiments in Polymer Science*, 1st ed, Wiley, New York, 1970, p 20
- 30 G V Vinogradov and A Ya Malkin, *Rheology of Polymers*, Mir, Moscow, 1980.
- 31 R Joseph, S Devi, and A K Rakshit, *Polym. Int*, **26**, 89 (1991)
- 32 A S Narang and U C Garg, *J Ind Chem Soc*, **66**, 214 (1989)
- 33 V Vangani and A K. Rakshit, *J Appl Polym Sci*, **45**, 1165 (1992)
- 34 R. Simha, *J Phys Chem*, **44**, 25 (1940).
- 35 H H Kohler and J Strand, *J Phys Chem*, **94**, 7628 (1990)
- 36 S Ajitkumar, D. Prasadkumar, S Kansara, and N K Patel, *Eur Polym J*, **31**, 149 (1995)